



## Thermal expansion of $(\text{Ca}_{1-x}\text{Pu}_x)\text{TiO}_3$

Tsuyoshi Sato<sup>a</sup>, Yutaka Hanajiri<sup>a</sup>, Toshiyuki Yamashita<sup>b</sup>, Tsuneo Matsui<sup>a,\*</sup>,  
Takanori Nagasaki<sup>a</sup>

<sup>a</sup> Department of Quantum Engineering, Graduate School of Engineering, Nagoya University, Furo-cho, Chikusa-ku, Nagoya 464-8603, Japan

<sup>b</sup> Department of Materials Science, Japan Atomic Energy Research Institute, Tokai, Ibaraki 319-1195, Japan

### Abstract

The phase relationship between  $\text{PuO}_{2-x}$  and  $\text{CaTiO}_3$  at room temperature was investigated by X-ray diffraction. It was found that Pu was soluble to at least 20 mol% in  $\text{CaTiO}_3$  in Ar–8%  $\text{H}_2$ . Solubility of Pu in  $\text{CaTiO}_3$  was extremely limited (below 5 mol%) under oxidizing condition. The thermal expansion of  $(\text{Ca}_{1-x}\text{Pu}_x)\text{TiO}_3$  ( $x = 0\text{--}0.15$ ) was investigated in the temperature range from room temperature to 1273 K by high-temperature X-ray diffraction. The linear thermal expansion coefficients showed considerable anisotropy for the orthorhombic  $Pbnm$  structure and decreased with increasing Pu content. The structural phase-transition temperatures were estimated from the lattice constants and were relatively insensitive to the content of Pu dopant. The estimated melting point increased with increasing Pu content, indicating that the thermodynamic stability of  $\text{CaTiO}_3$  increased with the addition of Pu. © 2001 Elsevier Science B.V. All rights reserved.

### 1. Introduction

The development of a safe disposal technique of high-level nuclear waste (HLW) is necessary for public acceptance in nuclear engineering. Perovskite oxides, such as  $\text{CaTiO}_3$ , have been recognized as one of the promising oxides for immobilization of HLW, since this oxide can form solid solutions with lanthanides and actinides. Transuranium (TRU) elements that have a long half-life in HLW, such as Pu, are thought to be incorporated in perovskite phases. Hence it is important to investigate the thermophysical properties of Pu-doped  $\text{CaTiO}_3$  in order to understand its stability at temperatures which will be encountered during preparation and storage of the waste form, in which Pu will be one of the major actinide nuclides.

It has been reported that the lanthanides and the actinides in waste mostly substitute for Ca in  $\text{CaTiO}_3$  [1]. The phase equilibria of  $\text{CaTiO}_3$  doped with Ce, Nd and U have been studied [2] by X-ray diffraction, where Ce, Nd and U were chosen to simulate TRU. The solubility

limit of Ce in  $\text{CaTiO}_3$  was between 20 and 30 mol% in purified argon, of Nd in  $\text{CaTiO}_3$  between 20 and 30 mol% in air, and of U in  $\text{CaTiO}_3$  between 0 and 3 mol% in purified argon [2]. The existence of trivalent Ce was confirmed in these doped samples by EXAFS measurements [3]. The solubility of lanthanides and actinides in  $\text{CaTiO}_3$  seems to be greatly dependent on the valence state of the dopant.

Pure  $\text{CaTiO}_3$  perovskite showed an anisotropic thermal expansion. The order was  $\alpha_a > \alpha_c > \alpha_b$  for the orthorhombic  $Pbnm$  structure [4–6]. Phase transitions of pure  $\text{CaTiO}_3$  were investigated by high-temperature X-ray diffraction [6]. The first transition (in the range 1373–1423 K) was due to the change from orthorhombic  $Pbnm$  to tetragonal  $I4/mcm$  structure, and the second one at  $1523 \pm 10$  K was from  $I4/mcm$  to cubic  $Pm\bar{3}m$  structure. Matsui et al. [7] re-investigated the phase transition of pure  $\text{CaTiO}_3$  and  $(\text{Ca}_{0.85}\text{Nd}_{0.15})\text{TiO}_3$  by high-temperature X-ray diffraction and differential thermal analysis. They found that the first transition at 1390 K was due to the change from orthorhombic  $Pbnm$  to orthorhombic  $Cmcm$  structure, and the second one at 1530 K from  $Cmcm$  to cubic  $Pm\bar{3}m$  structure.

In the present paper, the phase relationship between  $\text{PuO}_{2-x}$  and  $\text{CaTiO}_3$ , and the thermal expansion of

\* Corresponding author. Tel.: +81-52 789 4682; fax: +81-52 789 4691.

E-mail address: t-matsui@nucl.nagoya-u.ac.jp (T. Matsui).

$(\text{Ca}_{1-x}\text{Pu}_x)\text{TiO}_3$  in the temperature range from room temperature to 1273 K, were investigated by X-ray diffraction. Attention was paid to the oxidation states of Pu which depended on heating atmospheres. The structural phase transition of  $(\text{Ca}_{1-x}\text{Pu}_x)\text{TiO}_3$  from orthorhombic to orthorhombic/tetragonal structure is discussed in relation to the anisotropic thermal expansions.

## 2. Experimental

### 2.1. Materials

Pure  $\text{PuO}_2$  was prepared as follows. Plutonium dioxide was dissolved in 7 M  $\text{HNO}_3$  at about 350 K. The solution was passed through an ion-exchange column of Dowex 1-X4 to remove  $^{241}\text{Am}$  impurities. Plutonium oxalate was precipitated from the solution by adding oxalic acid, and then heated in air at about 1200 K to decompose the oxalate to  $\text{PuO}_2$  powder.

$\text{CaCO}_3$  and  $\text{TiO}_2$ , supplied by Rare Metallic Co., Tokyo, were 99.99% pure. These powders were weighed and mixed, then pressed into pellets under a pressure of 300 MPa without binder. The compositions prepared in this study were  $(\text{Ca}_{1-x}\text{Pu}_x)\text{TiO}_3$ :  $x = 0, 0.05, 0.10, 0.15,$  and  $0.20$ . The samples were heated in air at 1773 K for about 6 h, vacuum (about  $3.3 \times 10^{-3}$  Pa) at 1773 K for about 6 h and Ar-8%  $\text{H}_2$  at 1673 K for about 6 h, and then pulverizing with an agate mortar and a pestle. The heating and pulverizing processes were repeated several times until the phase equilibrium was attained. The products were ground in an agate mortar and subjected to X-ray diffraction analysis.

### 2.2. X-ray diffraction study

The high-temperature X-ray diffraction study was carried out using a Rigaku RAD-3C diffractometer system attached to a Rigaku furnace unit. The vacuum housing and a Pt heating element allowed examination in controlled atmospheres of He-8%  $\text{H}_2$  gas at high temperatures. Furnace temperature was measured by an R-type thermocouple inserted into a thin hole of a sample holder and was controlled by a PID-type temperature controller to within  $\pm 1$  K during X-ray measurements. In order to recover lattice distortion in crystallites caused by self-radiation damage, each specimen was first heated at 1273 K for 1 h in He-8%  $\text{H}_2$  before the X-ray measurements were made. Then the furnace temperature was decreased by 50 or 100 K and kept at this temperature for an hour, and then the X-ray measurements were carried out. This procedure was repeated down to room temperature. A detailed description of the high-temperature X-ray diffraction method was given in a previous paper [8].

X-ray diffraction patterns were recorded in the range from  $2\theta = 20$ – $130^\circ$  at temperatures between room temperature and 1273 K in He-8%  $\text{H}_2$ . Because of poor peak profiles at high angles, lattice parameters were calculated using reflections in the range of  $20^\circ < 2\theta < 80^\circ$  employing the least-squares method for the Nelson–Riley extrapolation [9]. The estimated error in lattice parameter was  $\pm 3.0 \times 10^{-4}$  nm.

## 3. Results and discussion

### 3.1. Phase relationships

The crystal structure of all  $(\text{Ca}_{1-x}\text{Pu}_x)\text{TiO}_3$  samples heated in Ar-8%  $\text{H}_2$  was orthorhombic, and lattice parameters of the samples are shown in Fig. 1 as a function of Pu content. In this figure, the lattice parameters  $a/\sqrt{2}$ ,  $b/\sqrt{2}$  and  $c/2$  are plotted. The relationship between the lattice parameter of the ideal cubic perovskite structure,  $a_{\text{ideal}}$ , and those of the orthorhombic  $Pbmm$  perovskite structure,  $a, b$  and  $c$ , is known to be  $a \cong \sqrt{2}a_{\text{ideal}}$ ,  $b \cong \sqrt{2}a_{\text{ideal}}$  and  $c \cong 2a_{\text{ideal}}$ . The lattice parameters,  $a, b$  and  $c$  were found to increase linearly with Pu content, showing that plutonium was soluble in  $\text{CaTiO}_3$  to at least 20 mol% in Ar-8%  $\text{H}_2$ . The solubility limit of Ce in  $\text{CaTiO}_3$  was determined to be between 20 and 30 mol% in purified argon [2] as mentioned before. Thus, the present result of Pu-doping is consistent with the earlier result for Ce-doping.

Doped  $\text{CaTiO}_3$  samples heated in air and vacuum showed the presence of the multi-phases of perovskite,  $\text{PuO}_2$  and  $\text{TiO}_2$ . The solubility of Pu in  $\text{CaTiO}_3$  was extremely limited (below 5 mol%) under oxidizing conditions. This agrees with the earlier result for  $\text{CaTiO}_3$

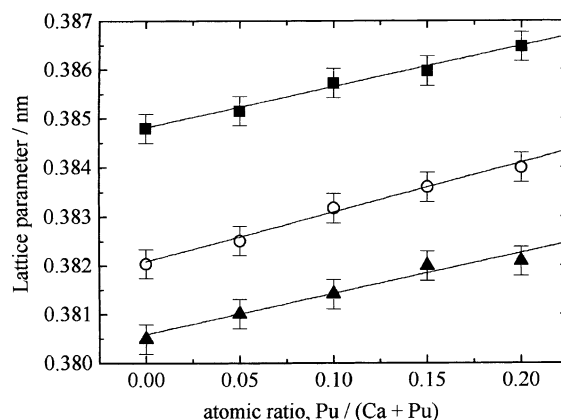


Fig. 1. Room temperature lattice parameters of  $(\text{Ca}_{1-x}\text{Pu}_x)\text{TiO}_3$  heated in Ar-8%  $\text{H}_2$  as a function of Pu content. ▲ –  $a/\sqrt{2}$ ; ■ –  $b/\sqrt{2}$ , ○ –  $c/2$ .

doped with Ce, where a single phase could not be formed by heating in air [2]. Under oxidizing conditions, Pu and Ce ions are considered to exist as tetravalent ions. The solubility of  $U^{4+}$  in  $CaTiO_3$  has been reported to be very limited in the oxidizing atmosphere in our previous study [2]. The low solubility of Pu in  $CaTiO_3$  in oxidizing atmospheres found in this study is in good agreement with these previous results.

Solubility in  $CaTiO_3$  is thought to be influenced mainly by the valence state and ionic radius of dopants with reference to those of  $Ca^{2+}$ . The ionic radii of trivalent Ce and Nd with 12 coordination numbers are 0.134 and 0.127 nm, respectively, which are comparable to that of  $Ca^{2+}$ , 0.134 nm [10]. On the other hand, the ionic radii of tetravalent Ce and U are 0.114 and 0.117 nm, respectively, and are about 10% smaller than that of  $Ca^{2+}$ . The ionic radii of  $Pu^{3+}$  and  $Pu^{4+}$  must be nearly the same as that of lanthanides with the corresponding valence state considering the similarity in chemical behavior. However, the ionic radii of  $Pu^{3+}$  and  $Pu^{4+}$  in 12-coordination are not available in the literature. Therefore, the limited solubility of tetravalent dopants in  $CaTiO_3$  may be caused by large differences in valence states and in ionic sizes compared with those of  $Ca^{2+}$ .

### 3.2. Thermal expansion

The lattice parameters of  $(Ca_{1-x}Pu_x)TiO_3$  at elevated temperatures were measured in He–8%  $H_2$ . Fig. 2 shows the variation of the lattice parameters with temperature. The lattice parameter for each specimen ( $x=0, 0.05, 0.10, \text{ and } 0.15$ ) increased smoothly with increasing temperature up to about 1300 K. Measured lattice parameters,  $a$ ,  $b$  and  $c$  were fitted as a function of temperature in the forms  $a(T)/\sqrt{2} = A_0 + A_1T$ ,  $b(T)/$

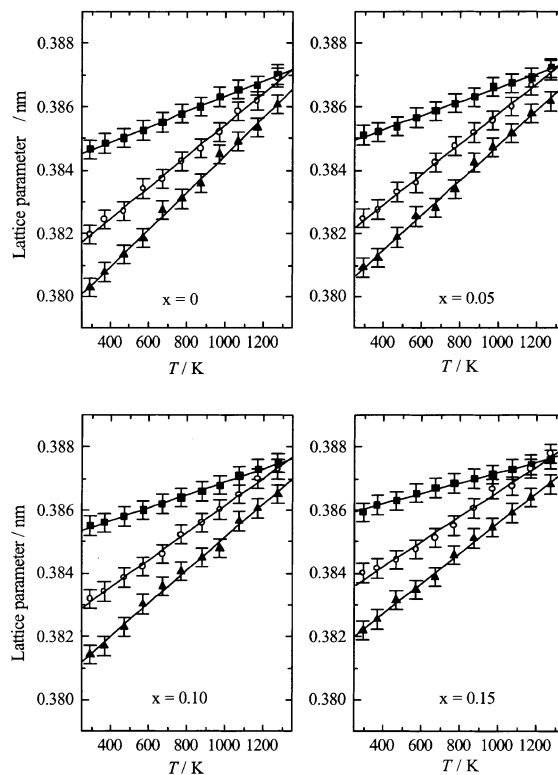


Fig. 2. Temperature dependence of lattice parameters of  $(Ca_{1-x}Pu_x)TiO_3$  in He–8%  $H_2$ . Regression results:  $\blacktriangle$  –  $a/\sqrt{2}$ ,  $\blacksquare$  –  $b/\sqrt{2}$ ,  $\circ$  –  $c/2$ ; solid lines indicate the regression results using data listed in Table 1.

$\sqrt{2} = B_0 + B_1T$  and  $c(T)/2 = C_0 + C_1T$ . The regression results are listed in Table 1. The linear thermal expansion coefficients of the  $a$ -,  $b$ - and  $c$ -axes calculated using the values in Table 1 are summarized in Table 2. The

Table 1

Regression data of lattice parameter for  $(Ca_{1-x}Pu_x)TiO_3^a$

$x$	$A_0$	$10^6 A_1$	$B_0$	$10^6 B_1$	$C_0$	$10^6 C_1$
0	0.3786	5.885	0.3839	2.416	0.3805	4.940
0.05	0.3793	5.511	0.3844	2.199	0.3810	4.781
0.10	0.3799	5.247	0.3848	2.078	0.3818	4.345
0.15	0.3808	4.761	0.3856	1.645	0.3826	3.987

<sup>a</sup>  $a(T)/\sqrt{2} = A_0 + A_1T$ ,  $b(T)/\sqrt{2} = B_0 + B_1T$ ,  $c(T)/2 = C_0 + C_1T$ .

Table 2

Linear expansion coefficient ( $10^6 K^{-1}$ ) of  $(Ca_{1-x}Pu_x)TiO_3^a$

$x$	Temp. range (K)	$\alpha_a$	$\alpha_b$	$\alpha_c$	$\alpha_v^*$
0	298–1273	$15.5 \pm 0.97$	$6.28 \pm 0.34$	$12.9 \pm 0.86$	$35.1 \pm 2.2$
0.05		$14.5 \pm 0.97$	$5.71 \pm 0.40$	$12.5 \pm 0.64$	$33.0 \pm 2.1$
0.10		$13.8 \pm 1.1$	$5.39 \pm 0.32$	$11.3 \pm 0.63$	$30.8 \pm 2.1$
0.15		$12.5 \pm 0.73$	$4.26 \pm 0.41$	$10.4 \pm 1.3$	$27.2 \pm 2.4$

<sup>a</sup>  $\alpha_v$  = volumetric thermal expansion coefficient.

thermal expansion of  $(\text{Ca}_{1-x}\text{Pu}_x)\text{TiO}_3$  shows a considerable anisotropic character. The calculated linear thermal expansion coefficient values,  $\alpha_a$ ,  $\alpha_b$ , and  $\alpha_c$  for orthorhombic  $Pbnm$  structure are in the order  $\alpha_a > \alpha_c > \alpha_b$ , which is of the same order as that of pure  $\text{CaTiO}_3$  [4–6].

The anisotropic thermal expansion of  $(\text{Ca}_{1-x}\text{Pu}_x)\text{TiO}_3$  induces structural phase transitions. Matsui et al. [7] have found the presence of two structural phase transitions from orthorhombic  $Pbnm$  to orthorhombic  $Cmcm$  at about 1390 K and from orthorhombic  $Cmcm$  to cubic  $Pm\bar{3}m$  around 1530 K by high-temperature X-ray diffraction. Kennedy et al. [11] have recently reported the presence of the transition from orthorhombic  $Pbnm$  to orthorhombic  $Cmcm$  at around 1380 K, and then to tetragonal  $I4/mcm$  structure near 1500 K and finally to cubic  $Pm\bar{3}m$  structure above 1580 K by neutron diffraction. The literature data on the crystal structures and transition temperatures of  $\text{CaTiO}_3$  [4–7,11] are summarized in Fig. 3.

As can be seen in Fig. 2, the regression lines for  $b/\sqrt{2}$  (filled squares) and  $c/2$  (open circles) appear to intersect around 1300–1350 K, suggesting the presence of a structural transition from orthorhombic to tetragonal. However, in the case of a transition from one orthorhombic to another orthorhombic structure, the lines for  $b/\sqrt{2}$  and  $c/2$  would approach (but not cross) as the temperature was increased. Subsequent crossing of the lines at a higher temperature would cause a transition from orthorhombic to tetragonal structure, as is seen in the data of Kennedy et al. [11]. Thus, the data in Fig. 2 are insufficient to give a precise determination of the transition temperature and the structural change.

The transition temperature has been also determined to be 1386 K from the heat capacity data for  $\text{CaTiO}_3$  doped with Nd [12] and 1380 K for  $\text{CaTiO}_3$  doped with Ce and La [13], showing a small influence on the transition temperature by doping to Ca site in  $\text{CaTiO}_3$ . In these reports, it was inferred that, in going from orthorhombic  $Pbnm$  to orthorhombic  $Cmcm$ , both the change in the interoctahedral rotation about one of the axes of

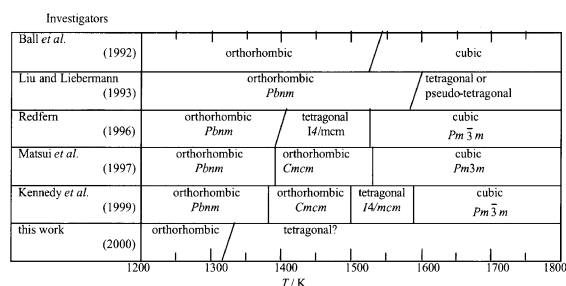


Fig. 3. Summary of the literature data on the transition temperatures and the crystal structures for several phase transitions of pure  $\text{CaTiO}_3$  [4–7,11].

Table 3

Estimated melting point of  $(\text{Ca}_{1-x}\text{Pu}_x)\text{TiO}_3$

$x$	$M_p$ (K)	$10^6\alpha_L$ ( $\text{K}^{-1}$ )
0	2262 (criterion)	11.7
0.05	$2388 \pm 140$	$11.0 \pm 0.7$
0.10	$2531 \pm 150$	$10.3 \pm 0.7$
0.15	$2826 \pm 150$	$9.11 \pm 0.8$

the  $\text{TiO}_6$  octahedra and the displacement of the Ca atoms surrounded by the eight  $\text{TiO}_6$  octahedra are small. The difference in the ionic radii between Ca and dopant atoms, Nd, Ce and La is also small and, hence, the result is not surprising. The small influence of Pu-doping in  $\text{CaTiO}_3$  on the transition temperature observed in the present study, therefore, is thought to be consistent with the previous results.

### 3.3. Estimation of melting point

As seen in Table 2, the linear thermal expansion coefficients of the  $a$ -,  $b$ - and  $c$ -axes decrease with increasing Pu content. Uiter et al. [14] pointed out that the average thermal expansion coefficient ( $\alpha_L$ ) decreased in inverse proportion to the melting point measured in  $^\circ\text{C}$ . That is,

$$\alpha_L(M_p - 273.15) = \text{const.}, \quad (1)$$

where  $M_p$  is the melting point (K). The melting temperature of  $(\text{Ca}_{1-x}\text{Pu}_x)\text{TiO}_3$  can, therefore, be estimated from Eq. (1). Since  $(\text{Ca}_{1-x}\text{Pu}_x)\text{TiO}_3$  showed anisotropic thermal expansion, the average thermal expansion coefficient was assumed to be equal to a third of the average volumetric thermal expansion coefficient:  $\alpha_L \cong \alpha_V/3$ . From the melting temperature,  $1989^\circ\text{C}$  of pure  $\text{CaTiO}_3$  and the  $\alpha_L$ ,  $11.7 \times 10^{-6} \text{ K}^{-1}$ , in this study, 'const' in Eq. (1) was evaluated as

$$\alpha_L(M_p - 273.15) = 0.0233. \quad (2)$$

The estimated melting temperatures for Pu-doped  $\text{CaTiO}_3$  are listed in Table 3, and increase with increasing Pu content. Thermal expansion coefficients and melting temperatures can be regarded as important measures of binding energy and, hence, thermodynamic stability. The present results showed clearly that the thermodynamic stability of  $\text{CaTiO}_3$  is increased by Pu substitution for Ca in  $\text{CaTiO}_3$ .

## 4. Conclusions

The phase relationship between  $\text{PuO}_{2-x}$  and  $\text{CaTiO}_3$  was investigated. It was found that Pu was soluble in  $\text{CaTiO}_3$  up to at least 20 mol% prepared in Ar–8%  $\text{H}_2$ , and that the solubility of Pu in  $\text{CaTiO}_3$  prepared in air and vacuum was extremely limited (below 5 mol%). The limited solubility of tetravalent dopants was attributed

to a large difference in valence state and ionic radius compared to those of  $\text{Ca}^{2+}$ .

The thermal expansion of  $(\text{Ca}_{1-x}\text{Pu}_x)\text{TiO}_3$  in the temperature range from room temperature to 1273 K was investigated by high-temperature X-ray diffraction. The lattice parameters of  $(\text{Ca}_{1-x}\text{Pu}_x)\text{TiO}_3$  increased smoothly with increasing temperature. The linear thermal expansion coefficients showed considerable anisotropy of  $\alpha_a$ ,  $\alpha_b$  and  $\alpha_c$  for orthorhombic *Pbnm* structure and decreased with increasing Pu content. The estimated structural phase-transition temperatures were insensitive to the content of Pu dopant. The estimated melting point increased with increasing Pu content, indicating that the thermodynamic stability of  $\text{CaTiO}_3$  increased by incorporation of Pu.

#### Acknowledgements

The authors would like to thank Dr Nakamura of JAERI for his encouragement and support to this work and also Dr H. Shigematsu of Nagoya University for valuable discussions on the structural phase transition. This work has been performed under the Joint Research Project between Japan Atomic Energy Research Institute and Universities on Backend Chemistry.

#### References

- [1] G.R. Lumpkin, K.J. Smith, M.G. Blackford, *J. Nucl. Mater.* 224 (1995) 131.
- [2] Y. Hanajiri, H. Yokoi, T. Matsui, Y. Arita, T. Nagasaki, H. Shigematsu, *J. Nucl. Mater.* 247 (1997) 285.
- [3] Y. Hanajiri, T. Matsui, Y. Arita, T. Nagasaki, H. Shigematsu, T. Harami, *Solid State Ionics* 108 (1998) 343.
- [4] C.J. Ball, G.J. Thorogood, E.R. Vance, *J. Nucl. Mater.* 190 (1992) 298.
- [5] X. Liu, R.C. Liebermann, *Phys. Chem. Miner.* 20 (1993) 171.
- [6] S.A.T. Redfern, *J. Phys. Condens. Matter* 8 (1996) 8267.
- [7] T. Matsui, H. Shigematsu, Y. Arita, Y. Hanajiri, N. Nakamitsu, T. Nagasaki, *J. Nucl. Mater.* 247 (1997) 72.
- [8] T. Yamashita, N. Nitani, T. Tsuji, H. Inagaki, *J. Nucl. Mater.* 245 (1997) 72.
- [9] J.B. Nelson, D.P. Riley, *Proc. Phys. Soc. London* 57 (1945) 160.
- [10] R.D. Shannon, *Acta Cryst. A* 32 (1976) 751.
- [11] B.J. Kennedy, C.J. Howard, B.C. Chakoumakos, *J. Phys. Condens. Matter* 11 (1999) 1479.
- [12] K. Nagarajan, Y. Arita, N. Nakamitsu, Y. Hanajiri, T. Matsui, *J. Nucl. Mater.* 230 (1996) 124.
- [13] Y. Arita, K. Nagarajan, T. Ohashi, T. Matsui, *J. Nucl. Mater.* 247 (1997) 94.
- [14] L.G. Van Uitert, H.M. O'Bryan, M.E. Lines, H.J. Guggenheim, G. Zyzik, *Mater. Res. Bull.* 12 (1977) 261.